Unpolarized and polarized quark distributions in the large-N_c limit

D. I. Diakonov
NORDITA, Blegdamsvej 17, 2100 Copenhagen Ø, Denmark

V. Yu. Petrov
Petersburg Nuclear Physics Institute, Gatchina, St. Petersburg 188350, Russia

P. V. Pobylitsa,* M. V. Polyakov,* and C. Weiss
Institut für Theoretische Physik II, Ruhr-Universität Bochum, D-44 780 Bochum, Germany
(Received 26 March 1997)

The isosinglet unpolarized and isovector polarized twist-2 quark distributions of the nucleon at low normalization point are calculated in the large-N_c limit. The nucleon is described as a soliton of the effective chiral theory. We derive the expressions for the distribution functions in the large-N_c limit starting from their definition as numbers of partons carrying a momentum fraction x in the infinite momentum frame. We develop a numerical method for computation of the quark and antiquark distributions as sums over the quark single-particle levels in the pion field of the soliton. The contributions of the discrete bound-state level as well as the Dirac continuum are taken into account. The quark and antiquark distributions obtained explicitly satisfy all general requirements. The results are in reasonable agreement with parametrizations of the data at a low normalization point. [S0556-2821(97)02817-8]

PACS number(s): 12.38.Lg, 12.39.Ki, 13.60.Hb

I. INTRODUCTION

The evolution of parton distributions with q^2 in the asymptotic region is well understood today, being governed by the renormalization group equation of perturbative QCD. A complete description of experiments at large q^2 requires, however, the knowledge of parton distributions in the nucleon at some initial normalization point. Several sets of input distributions were determined by fits to the experimental data at large q^2 [1–4]. All these fits include antiquarks and gluons at a low normalization point.

Recently, we have formulated an approach to calculate the twist-2 parton distributions at low normalization point in the limit of a large number of colors (N_c), where the nucleon is described as a chiral soliton [5]. At low energies, QCD may be approximated by an effective theory whose degrees of freedom are quarks with a dynamically generated mass, interacting with pions, which appear as Goldstone bosons of the dynamically broken chiral symmetry. The nucleon emerges as a classical soliton of the pion field [6]. This picture is known to give a successful description of hadronic observables such as the nucleon mass, magnetic moments, form factors, etc. [7]. In [5] we have shown that this approach possesses all necessary requisites for a successful description of the leading-twist parton distributions of the nucleon. The normalization point of the distribution functions obtained in this way is of the order of the ultraviolet cutoff of the effective chiral theory, typically ~ 600 MeV. Let us briefly summarize the main characteristics of this description [5].

(i) *Classification of quark distributions in the large-N_c limit.* In the large-N_c limit the quark distributions are concentrated at values of $x \sim 1/N_c$. Combining this fact with the known large-N_c behavior of the integrals of the distributions over x, one infers that the quark distributions in the large-N_c limit can be divided in ''large'' and ''small'' ones. The leading distributions are the isosinglet unpolarized and isovector polarized distributions, which are of the form

$$D^{\text{large}}(x) \sim N_c^2 \rho(N_c x), \tag{1}$$

where $\rho(y)$ is a stable function in the large-N_c limit, which depends on the particular distribution considered. The isovector unpolarized and isosinglet polarized distributions appear only in the next-to-leading order of the $1/N_c$ expansion, and are of the form

$$D^{\text{small}}(x) \sim N_c \rho(N_c x). \tag{2}$$

(ii) *Sum rules and antiquark distributions.* The chiral soliton model is a field-theoretic description of the nucleon, which preserves all general requirements on parton distributions. In particular, the standard sum rules for parton distributions and their positivity properties are satisfied automatically within the model. Also, a consistent description of the antiquark distributions can be achieved in this approach.

(iii) *Parametric smallness of the gluon distribution.* When working with the effective chiral theory, it is implied that the ratio of the dynamical quark mass, M, to the UV cutoff, Λ (not to be confused with the QCD scale parameter, Λ_{QCD}), is parametrically small. For $M/\Lambda \ll 1$, the quark distributions computed in the effective theory may be identified with the ''current'' quark distributions of QCD. The gluon distribution is zero at this level, more precisely, it is $O(M^2/\Lambda^2)$. For finite M/Λ, the quark distributions computed in the effective theory should be interpreted as distributions of ''constitu-

*Permanent address: Petersburg Nuclear Physics Institute, Gatchina, St. Petersburg 188350, Russia.

ent'' quarks — objects which themselves have a substructure in terms of QCD partons. The gluon distribution inside these objects could in principle be recovered from the effective theory if one knew the precise way how the UV cutoff arises as a result of integration over the original QCD degrees of freedom. These statements can be made more precise in the framework of the instanton vacuum, which on one hand allows to derive the effective chiral theory, and on the other hand can be used to evaluate the gluon distribution directly, using the method developed in [8]. One finds that the gluon distribution is suppressed relative to the quark distributions by a factor of the packing fraction of the instanton medium [5].

In this paper, we study the properties of the N_c-leading quark and antiquark distributions, namely the isosinglet unpolarized and isovector polarized distributions, in the approach formulated in [5]. First, we rederive the basic formulas for the parton distributions in the effective chiral theory in a new way. In [5] these formulas were obtained from the exact QCD expressions for the parton distributions as matrix elements of quark bilinears with a lightlike separation [9,10]. In this paper we take the original Feynman point of view [11] that parton distributions are given by the number of partons carrying a fraction x of the nucleon momentum in the nucleon infinite-momentum frame. Despite the apparent difference in wording we show here that the two definitions are, in fact, equivalent and lead to identical working formulas for computing parton distributions. We think it is remarkable that the actual equivalence of the two well-known definitions can explicitly be demonstrated within this field-theoretical model of the nucleon. The deep reason for the equivalence is that the main hypothesis of the Feynman parton model, namely that partons transverse momenta do not grow with q^2 [11], is satisfied in the model under consideration.

Second, we investigate the influence of the ultraviolet cutoff of the effective chiral theory on the distribution functions. This not only includes the asymptotic dependence on the cutoff parameter (i.e., the UV divergences), but also, and more importantly, the dependence on the regularization scheme adopted to make the distributions finite. It is crucial that the regularization method not violate the completeness of quark single-particle states in the background pion field, in order to preserve causality, that is, the anticommutation relations of quark fields at spacelike separations. A regularization which meets this requirement is, for example, the Pauli-Villars subtraction. We show explicitly that it leads to quark and antiquark distribution functions satisfying all general requirements, such as rapid decrease for large x, uniform logarithmic dependence on the cutoff, and positivity. On the other hand, regularization methods based on an energy cutoff, such as the popular proper-time regularization of the determinant, violate causality and lead to unacceptable results for the distribution functions.

Third, we develop a numerical method for exact computation of the quark and antiquark distribution functions as sums over quark single-particle levels in the background pion field. (In [5] the polarized distributions were estimated using an approximation, the so-called interpolation formula.) Since the quark distribution functions are given by matrix elements of products of quark fields at finite time and space separations, their computation requires evaluation of functional traces of the single-particle energy and momentum operator, which is in general a difficult problem. Using the finite-basis method of [12], we formulate a reliable and efficient numerical procedure to compute the Pauli-Villars regularized quark and antiquark distributions. The method takes into account the contributions of the discrete bound-state level as well as the Dirac continuum of quarks.

Finally, using the methods developed in this paper, we compute the isosinglet unpolarized and isovector polarized distribution functions and discuss the results. In principle, the resulting distributions should be taken as the starting point for perturbative evolution and be compared with structure function data at large q^2. The evolution of the calculated distributions and the comparison with the data will be the subject of a separate investigation. Here, we restrict ourselves to a comparison of the calculated distributions with the parametrizations of the data at a low normalization point by Glück and co-workers [3,4].

II. QUARK DISTRIBUTION FUNCTIONS IN THE LARGE-N_c LIMIT

A. The nucleon in the effective chiral theory

In the large-N_c limit, QCD becomes equivalent to an effective theory of mesons, with baryons emerging as solitonic excitations [13,14]. At low energies, the main guiding principle for formulating this effective theory is the dynamical breaking of chiral symmetry, which, in particular, results in the appearance of pions as Goldstone bosons. In the long-wavelength limit, the effective theory can be expressed in the form of the chiral Lagrangian of the pion field, whose structure is basically determined by chiral symmetry. The minimal chirally invariant interaction of quarks with Goldstone bosons is described by the functional integral [15–17]

$$\exp(iS_{\rm eff}[\pi(x)]) = \int D\psi D\overline{\psi} \exp\left(i \int d^4x\, \overline{\psi}(i\partial\!\!\!/ - MU^{\gamma_5})\psi \right). \tag{3}$$

Here, $\pi(x)$ is the pion field,

$$U(x) = \exp[i\pi^a(x)\tau^a], \tag{4}$$

$$U^{\gamma_5}(x) = \exp[i\pi^a(x)\tau^a\gamma_5] = \frac{1+\gamma_5}{2}U(x) + \frac{1-\gamma_5}{2}U^\dagger(x). \tag{5}$$

The quark field possesses a dynamical mass, M, due to chiral symmetry breaking. It is understood that, generally, this theory of massive quarks is valid up to an UV cutoff, $\Lambda \gg M$. The effective action Eq. (5) can be derived from the instanton vacuum, where the cutoff is determined by the inverse instanton size, and the dynamical quark mass is momentum dependent. In practice, rather than working with an explicitly momentum-dependent quark mass, one usually takes a constant quark mass and applies an UV cutoff to divergent quantities derived from Eq. (3), using some regularization scheme.

In the effective chiral theory defined by Eq. (3), the nucleon is in the large-N_c limit described by a static classical pion field. In the nucleon rest frame it is of ''hedgehog'' form [6]

$$U_c(\mathbf{x})=\exp[i(\mathbf{n}\cdot\boldsymbol{\tau})P(r)],$$

$$r=|\mathbf{x}|,$$

$$\mathbf{n}=\frac{\mathbf{x}}{r}. \tag{6}$$

Here, $P(r)$ is the profile function, with $P(0)=-\pi$ and $P(r)\to 0$ for $r\to\infty$, which is determined by minimizing the static energy of the pion field. Quarks are described by means of one-particle wave functions, to be found from the Dirac equation in the external pion field,

$$(i\gamma^\mu\partial_\mu - MU^{\gamma_5})\Psi_n(\mathbf{x},t)=0,$$

$$\Psi_n(\mathbf{x},t)=\exp(-iE_nt)\Phi_n(\mathbf{x}), \tag{7}$$

which can be written in Hamiltonian form:

$$H\Phi_n=E_n\Phi_n,$$

$$H=-i\gamma^0\gamma^k\partial_k+M\gamma^0U^{\gamma_5}. \tag{8}$$

The spectrum of the one-particle Hamiltonian, H, contains a discrete bound-state level. This level must be occupied by N_c quarks to have a state of unit baryon number. The nucleon mass is given by the minimum of the bound-state energy and the aggregate energy of the negative Dirac continuum, the energy of the free Dirac continuum subtracted [6]:

$$M_N=N_cE_{\rm lev}+N_c\sum_{E_n<0}(E_n-E_n^{(0)}). \tag{9}$$

[$E_n^{(0)}$ denotes the energy levels of the vacuum Hamiltonian given by Eq. (8) with $U=1$.] It is understood that Eq. (9) is made finite by some regularization method, to be discussed below.

Nucleon states of definite spin-isospin and 3-momentum are obtained by quantizing the rotational and translational zero modes of the soliton [their contributions to the energy are $O(1/N_c)$], by integrating over the corresponding collective coordinates with appropriate wave functions [6,7].

B. Quark distribution functions in the effective chiral theory

The simplest way to determine the quark distributions inside the nucleon is to use the infinite momentum frame and calculate the number of partons there [11]. It is well known that the infinite momentum helps to separate quarks belonging to the nucleon from the vacuum ones, provided that the transverse momenta of the particles are not growing with the nucleon momentum [11]. In our chiral quark soliton model this condition is, of course, satisfied.

More precisely, the quark distributions as functions of the Bjorken variable x are, by definition, the number of (anti) quarks whose momentum, say, in the z direction, is a fraction x of the nucleon momentum P_N in the infinite momentum frame where

$$P_N=\frac{M_Nv}{\sqrt{1-v^2}},\quad v\to 1. \tag{10}$$

The number of (anti) quarks can be expressed through the nucleon matrix element of the creation and annihilation operators, a^+,a (for quarks), and b^+,b (for antiquarks). We define the quark and antiquark distribution functions as

$$D_i(x)=\int\frac{d^3k}{(2\pi)^3}\,\delta\!\left(x-\frac{k^3}{P_N}\right)\langle N_{\mathbf{v}}|a_i^+(\mathbf{k})a_i(\mathbf{k})|N_{\mathbf{v}}\rangle, \tag{11}$$

$$\overline{D_i}(x)=\int\frac{d^3k}{(2\pi)^3}\,\delta\!\left(x-\frac{k^3}{P_N}\right)\langle N_{\mathbf{v}}|b_i^+(\mathbf{k})b_i(\mathbf{k})|N_{\mathbf{v}}\rangle. \tag{12}$$

Here i denotes the set of quantum numbers characterizing the quark, such as flavor and polarization.

In the infinite momentum frame it is possible to express these matrix elements in terms of the quark field operator

$$\psi(\mathbf{x},t)=\int\frac{d^3k}{(2\pi)^3\sqrt{2k_0}}\sum_c\,[a_c(\mathbf{k})\exp(-ik\cdot x)u_c(\mathbf{k}) + b_c^+(\mathbf{k})\exp(ik\cdot x)v_c(\mathbf{k})], \tag{13}$$

where $u(\mathbf{p})$, $v(\mathbf{p})$ are the wave function of the free quarks and antiquarks, normalized to $\overline{u}u=-\overline{v}v=2M$, and $c=1,2$ denotes the polarization. Let us consider the Fourier transform of the equal-time product of ψ and ψ^+:

$$\begin{aligned}\int d^3x_1d^3x_2\exp[-i\mathbf{k}\cdot(\mathbf{x}_1-\mathbf{x}_2)]\psi^+(\mathbf{x}_2,t)\psi(\mathbf{x}_1,t)\\ =\sum_{c,c'}\frac{1}{2k_0}[a_c^+(\mathbf{k})a_{c'}(\mathbf{k})u_c^*(\mathbf{k})u_{c'}(\mathbf{k})+a_c^+(\mathbf{k})b_{c'}^+(-\mathbf{k})\\ \times u_c^*(\mathbf{k})v_{c'}(-\mathbf{k})\exp(2ik^0t)+b_c(-\mathbf{k})a_{c'}(\mathbf{k})v_{c'}^*(-\mathbf{k})\\ \times u_c(\mathbf{k})\exp(-2ik^0t)+b_c(-\mathbf{k})b_{c'}^+(-\mathbf{k})v_c^*(-\mathbf{k})\\ \times v_{c'}(-\mathbf{k})].\end{aligned} \tag{14}$$

Averaging this operator over the nucleon state in the infinite momentum frame, with $k^3=xM_Nv/\sqrt{1-v^2}$, $v\to 1$, we get zero for all terms on the right-hand side (RHS) but the first one. Indeed, the probability to find a correlated quark-antiquark pair with very large opposite momenta (the second and third terms) in a fast moving nucleon goes to zero as $v\to 1$. Similarly, the probability to find antiquarks moving in the opposite direction to the nucleon with large longitudinal momenta goes to zero as $v\to 1$ (the fourth term). To be more precise, these matrix elements decrease with the nucleon momentum and can, in principle, contribute to the structure functions of nonleading twists. However, we are interested in the leading-twist distribution functions, and can therefore neglect all terms in Eq. (14) except the first one. The distri-

bution functions can thus be expressed in terms of equal-time products of the field operators as

$$D_i(x)=\int \frac{d^3k}{(2\pi)^3}\,\delta\!\left(x-\frac{k^3}{P_N}\right)\int d^3x_1 d^3x_2 \times\exp[-i\mathbf{k}\cdot(\mathbf{x}_1-\mathbf{x}_2)]\langle N_{\mathbf{v}}|\,\overline{\psi}(\mathbf{x}_2,t)\Gamma_i\psi(\mathbf{x}_1,t)|N_{\mathbf{v}}\rangle, \tag{15}$$

$$\overline{D_i}(x)=\int \frac{d^3k}{(2\pi)^3}\,\delta\!\left(x-\frac{k^3}{P_N}\right)\int d^3x_1 d^3x_2 \times\exp[-i\mathbf{k}\cdot(\mathbf{x}_1-\mathbf{x}_2)] \times\langle N_{\mathbf{v}}|\mathrm{Tr}[\Gamma_i\psi(\mathbf{x}_2,t)\,\overline{\psi}(\mathbf{x}_1,t)]|N_{\mathbf{v}}\rangle. \tag{16}$$

The flavor and spin matrices, Γ_i, depend on the particular distribution one is interested in. For example, for the number of partons polarized along or against the direction of the nucleon velocity one should use

$$\Gamma_i=\gamma^0\frac{1\pm\gamma_5}{2}, \tag{17}$$

respectively.

In order to evaluate the equal-time matrix elements in the nucleon state in Eqs. (15) and (16) we consider the more general matrix element of the *time-ordered* product of quark fields. In the effective chiral theory, this nucleon matrix element can directly be computed as a functional integral over the quark and pion field with the effective action, Eq. (3). At $N_c\to\infty$, the integral can be performed using the saddle point method [6]. One finds that

$$-i\langle N_{\mathbf{v}}|\mathrm{T}\{\psi(\mathbf{x}_1,t_1)\,\overline{\psi}(\mathbf{x}_2,t_2)\}|N_{\mathbf{v}}\rangle=G_F(x_1,x_2), \tag{18}$$

where $G_F(x_1,x_2)$ is the Feynman Green function in the background pion field corresponding to the moving nucleon. This saddle point solution of the classical equations of motion can easily be constructed. Indeed, since the saddle point equations are relativistically invariant, it is evident that the pion field is of the form

$$\hat{U}_c(\mathbf{x},t)=U_c\!\left(\frac{\mathbf{x}-\mathbf{v}t}{\sqrt{1-v^2}}\right), \tag{19}$$

where $U_c(\mathbf{x})$ is the stationary hedgehog pion mean field in the nucleon rest frame. The Feynman Green function, Eq. (18), is thus determined as the solution of the inhomogeneous Dirac equation

$$\left[i\gamma^\mu\frac{\partial}{\partial x_1^\mu}-M\hat{U}^{\gamma_5}(\mathbf{x}_1,t_1)\right]G_F(\mathbf{x}_1,t_1,\mathbf{x}_2,t_2)=\delta^{(4)}(x_1-x_2), \tag{20}$$

$$\hat{U}^{\gamma_5}(\mathbf{x},t)=\frac{1+\gamma_5}{2}\hat{U}_c(\mathbf{x},t)+\frac{1-\gamma_5}{2}\hat{U}_c^\dagger(\mathbf{x},t). \tag{21}$$

With Eq. (18), the distribution functions, Eqs. (15) and (16), can now be written in terms of the Feynman Green function as limits at $t_2\to t_1\pm 0$:

$$D_i(x)=-iN_c\int \frac{d^3k}{(2\pi)^3}\,\delta\!\left(x-\frac{k^3}{P_N}\right)\int d^3x_1 d^3x_2 \times\exp[-i\mathbf{k}\cdot(\mathbf{x}_1-\mathbf{x}_2)] \times\mathrm{Tr}[\Gamma_i G_F(\mathbf{x}_1,t_1,\mathbf{x}_2,t_2)]_{t_2=t_1+0}, \tag{22}$$

$$\overline{D_i}(x)=iN_c\int \frac{d^3k}{(2\pi)^3}\,\delta\!\left(x-\frac{k^3}{P_N}\right)\int d^3x_1 d^3x_2 \times\exp[-i\mathbf{k}\cdot(\mathbf{x}_1-\mathbf{x}_2)] \times\mathrm{Tr}[\Gamma_i G_F(\mathbf{x}_1,t_1,\mathbf{x}_2,t_2)]_{t_1=t_2+0}. \tag{23}$$

To compute the quark and antiquark distribution functions one needs an explicit representation of the Feynman Green function in the background pion field corresponding to the fast-moving nucleon. We now want to demonstrate that this Green function can be expressed in terms of the single-particle quark wave functions, $\Phi_n(\mathbf{x})$, and energy eigenvalues, E_n, in the nucleon rest frame, Eq. (7). The quark eigenfunctions in the time-dependent pion field, Eq. (19), can be obtained from the ones in the static pion field in the rest frame by a Lorentz transformation. We can thus write a representation of the Feynman Green function as

$$\begin{aligned}&G_F(\mathbf{x}_1,t_1,\mathbf{x}_2,t_2)\\ &=-iS[\mathbf{v}]\Bigg\{\theta(t_1-t_2)\sum_{\text{nonoccup}}\Phi_n(\mathbf{x}_1')\overline{\Phi}_n(\mathbf{x}_2')\\ &\times\exp[-iE_n(t_1'-t_2')]-\theta(t_2-t_1)\\ &\times\sum_{\text{occup}}\Phi_n(\mathbf{x}_1')\overline{\Phi}_n(\mathbf{x}_2')\exp[-iE_n(t_1'-t_2')]\Bigg\}S^{-1}[\mathbf{v}].\end{aligned} \tag{24}$$

Here t' and $\mathbf{x}'$ are the Lorentz transforms of the coordinates,

$$\mathbf{x}_{1,2}'=\frac{\mathbf{x}_{1,2}-\mathbf{v}t_{1,2}}{\sqrt{1-\mathbf{v}^2}},$$

$$t_{1,2}'=\frac{t_{1,2}-\mathbf{v}\cdot\mathbf{x}_{1,2}}{\sqrt{1-\mathbf{v}^2}}, \tag{25}$$

and $S[\mathbf{v}]$ is the Lorentz transformation matrix acting on the quark spinor indices,

$$S[\mathbf{v}]=\exp\!\left(\frac{i}{2}\sigma_{03}\omega\right),$$

$$\sigma_{\mu\nu}=\frac{i}{2}[\gamma_\mu,\gamma_\nu],$$

$$\tanh(\omega)=v. \tag{26}$$

In the first term of Eq. (24) the summation goes over nonoccupied states, that is over the positive-energy Dirac continuum, in the second term over occupied states, that is, over the negative continuum and the discrete bound-state level.

Let us prove that the Green function defined by Eq. (24) indeed satisfies the inhomogeneous Dirac equation, Eq. (20). We first note that the Lorentz transformed single-particle wave functions, $S[\mathbf{v}]\Phi_n(\mathbf{x}')\exp(-iE_nt')$, satisfy the homogeneous Dirac equation, Eq. (20) with RHS equal to zero, therefore so does the Green function, Eq. (24), at $t_1\neq t_2$. At $t_1=t_2$ the Green function has a discontinuity. Taking the time derivative of Eq. (24) at $t_1=t_2$ we find that the LHS of Eq. (20) is equal to $F(\mathbf{x}_1,\mathbf{x}_2)\delta(t_1-t_2)$, where

$$F(\mathbf{x}_1,\mathbf{x}_2)=\sum_{\text{all}}\exp[-iE_n\mathbf{v}(\mathbf{x}_1'-\mathbf{x}_2')]\gamma^0 S\Phi_n(\mathbf{x}_1')\overline{\Phi_n}(\mathbf{x}_2')S^{-1}. \tag{27}$$

This function should be equal to $\delta^{(3)}(\mathbf{x}_1-\mathbf{x}_2)$ in order to satisfy the inhomogeneous Dirac equation, Eq. (20), for the Green function.[1] To prove this, we first convince ourselves that the sum, Eq. (27), vanishes for $\mathbf{x}_1\neq\mathbf{x}_2$, and then show that it is indeed a delta function with coefficient unity.

We introduce temporarily two moments of ''time,'' $\tilde{t}_1=\mathbf{v}\mathbf{x}_1'$ and $\tilde{t}_2=\mathbf{v}\mathbf{x}_2'$, and note that at $\tilde{t}_1>\tilde{t}_2$, Eq. (27) can be written via the ''retarded'' Green function,

$$F(\mathbf{x}_1,\mathbf{x}_2)=i\gamma^0 S G_{\text{ret}}(\mathbf{x}_1',(\mathbf{v}\mathbf{x}_1'),\mathbf{x}_2',(\mathbf{v}\mathbf{x}_2'))S^{-1},$$

$$G_{\text{ret}}(\mathbf{x}_1',\tilde{t}_1,\mathbf{x}_2',\tilde{t}_2)=-i\theta(\tilde{t}_1-\tilde{t}_2)\sum_{\text{all}}\overline{\Phi_n}(\mathbf{x}_2')\Phi_n(\mathbf{x}_1')\times\exp[-iE_n(\tilde{t}_1-\tilde{t}_2)]. \tag{28}$$

We need this function in the spacelike region, since $(\tilde{t}_1-\tilde{t}_2)^2-(\mathbf{x}_1'-\mathbf{x}_2')^2=(\mathbf{v}\cdot(\mathbf{x}_1'-\mathbf{x}_2'))^2-(\mathbf{x}_1'-\mathbf{x}_2')^2<0$, at least when $\mathbf{x}_1\neq\mathbf{x}_2$. However, the retarded Green function is zero in the spacelike region. This is obvious from physical considerations: the retarded Green function determines the evolution of a wave packet which at $\tilde{t}_1=\tilde{t}_2$ is localized at $\mathbf{x}_1'=\mathbf{x}_2'$, which cannot reach the spacelike region. More formally, this can also be proved using the perturbation expansion for the retarded Green function in the external pion field:

$$G_{\text{ret}}(\mathbf{x}_1',\tilde{t}_1,\mathbf{x}_2',\tilde{t}_2)=G^0_{\text{ret}}(\mathbf{x}_1',\tilde{t}_1,\mathbf{x}_2',\tilde{t}_2)+\int d^3x_3'd\tilde{t}_3\times G^0_{\text{ret}}(\mathbf{x}_1',\tilde{t}_1,\mathbf{x}_3',\tilde{t}_3)MU^{\gamma_5}(\mathbf{x}_3')\times G^0_{\text{ret}}(\mathbf{x}_3',\tilde{t}_3,\mathbf{x}_2',\tilde{t}_2)+\cdots. \tag{29}$$

The free retarded Green function, G^0_{ret}, is zero for spacelike separations, therefore the second term is nonzero only for $\tilde{t}_1-\tilde{t}_3>|\mathbf{x}_1'-\mathbf{x}_2'|$ and for $\tilde{t}_3-\tilde{t}_2>|\mathbf{x}_2'-\mathbf{x}_3'|$. This implies that it is nonzero only for $\tilde{t}_1-\tilde{t}_2>|\mathbf{x}_1'-\mathbf{x}_3'|+|\mathbf{x}_3'-\mathbf{x}_2'|>|\mathbf{x}_1'-\mathbf{x}_2'|$. This argument is easily generalized to any term of the perturbation expansion.

Thus $F(\mathbf{x}_1,\mathbf{x}_2)$ is zero for $\mathbf{x}_1\neq\mathbf{x}_2$. It therefore must be proportional to a delta function in $\mathbf{x}_1-\mathbf{x}_2$ or its derivatives. This ''point'' singularity can come only from states with large energies, E_n. For such states, one can neglect the pion field and replace the wave functions, $\Phi_n(\mathbf{x})$, by the eigenfunction of the free Hamiltonian. Saturating the sum in the RHS of Eq. (28) by plane waves we obtain

$$F(\mathbf{x}_1,\mathbf{x}_2)=\delta^{(3)}(\mathbf{x}_1-\mathbf{x}_2). \tag{30}$$

(In other words, the leading short-distance singularity of the Green function in the background pion field is the same as that of the free Green function.) This completes the proof that Eq. (24) is a representation of the Feynman Green function in the time-dependent background field, Eq. (20).

We now use the representation, Eq. (24), to express the distribution functions directly through the quark wave functions in the nucleon rest frame. Passing to the Fourier transforms of the quark wave functions, integrating in Eqs. (22) and (23) over $\mathbf{x}_{1,2}$, and taking the limit $v\to1$, we finally obtain

$$D_i(x)=N_cM_N\sum_{\text{occup}}\int\frac{d^3k}{(2\pi)^3}\Phi_n^\dagger(\mathbf{k})(1+\gamma^0\gamma^3)\times\gamma^0\Gamma_i\delta(k^3+E_n-xM_N)\Phi_n(\mathbf{k}), \tag{31}$$

$$\overline{D_i}(x)=N_cM_N\sum_{\text{nonoccup}}\int\frac{d^3k}{(2\pi)^3}\Phi_n^\dagger(\mathbf{k})(1+\gamma^0\gamma^3)\times\gamma^0\Gamma_i\delta(k^3+E_n+xM_N)\Phi_n(\mathbf{k}). \tag{32}$$

These formulas represent the quark distributions as sums over occupied states, the antiquark distributions as sums over nonoccupied states. We can also write an alternative representation for the distribution functions, using the time-ordering opposite to the one in Eqs. (22) and (23), and the fact that the discontinuity of the Feynman Green function is a space δ function. In this case we get

$$D_i(x)=-N_cM_N\sum_{\text{nonoccup}}\int\frac{d^3k}{(2\pi)^3}\Phi_n^\dagger(\mathbf{k})(1+\gamma^0\gamma^3)\times\gamma^0\Gamma_i\delta(k^3+E_n-xM_N)\Phi_n(\mathbf{k}), \tag{33}$$

$$\overline{D_i}(x)=-N_cM_N\sum_{\text{occup}}\int\frac{d^3k}{(2\pi)^3}\Phi_n^\dagger(\mathbf{k})(1+\gamma^0\gamma^3)\times\gamma^0\Gamma_i\delta(k^3+E_n+xM_N)\Phi_n(\mathbf{k}). \tag{34}$$

In both Eqs. (31) and (32) and Eqs. (33) and (34) it is understood that the contribution of free quarks is to be subtracted. In the original representation of the distribution functions through the Feynman Green function, Eqs. (22) and (23), this means that the leading short-distance singularity of the Green function in the background pion field is canceled by the one of the free Green function, cf. Eq. (30). However, Eqs. (31) and (32) and Eqs. (33) and (34) still contain ultra-

[1] In field theory, Eq. (27) represents the equal-time anticommutator, $\{\psi(\mathbf{x}_1,t),\psi^+(\mathbf{x}_2,t)\}=\delta^{(3)}(\mathbf{x}_1-\mathbf{x}_2)$.

violet divergences and have to be made finite by some regularization scheme, to be discussed in Sec. III.

It is clear that the equivalence of the representations of the distribution functions as sums over occupied and nonoccupied states, Eqs. (31) and (32) and Eqs. (33) and (34), is based on the completeness of quark states in the external pion field, Eq. (30), which can in principle be violated by ultraviolet regularization. Fortunately, it is possible to regularize the theory in such a way that this important property is preserved; see Sec. III.

We emphasize that the expressions in Eqs. (31) and (32) and Eqs. (33) and (34) are identical to those which have been derived in Ref. [5] from a representation of the distribution functions as nucleon matrix elements of quark bilinears separated by a lightlike distance. The above derivation is a demonstration of the equivalence of the two definitions of parton distributions.

Finally, to get the unpolarized or polarized (anti) quark distributions corresponding to a nucleon state of definite spin and isospin, one has to take the desired combinations of the basic expressions, Eqs. (31) and (32), and average them with the nucleon spin-isospin wave function (the procedure is described in [5]). In this paper we consider the distributions which appear in the leading order of the $1/N_c$ expansion, the isosinglet unpolarized and the isovector polarized one. To obtain the isosinglet unpolarized quark distribution we sum up the two polarizations in Eq. (31) and average over flavor. One finds [5]

$$[u(x)+d(x)]_{\rm occup}=N_cM_N\sum_{\substack{n\\ \rm occup}}\int\frac{d^3k}{(2\pi)^3}\Phi_n^\dagger(\mathbf{k})(1+\gamma^0\gamma^3)\times\delta(k^3+E_n-xM_N)\Phi_n(\mathbf{k}). \tag{35}$$

From Eq. (34) one sees that the corresponding antiquark distribution can also be written as a sum over occupied states; it is given by the negative of the RHS of Eq. (35) at $x\to -x$. Henceforth, we shall consider Eq. (35) as a function defined for both positive and negative x, and understand that at negative x it describes minus the antiquark distribution. Alternatively, we can use Eqs. (32) and (33) to obtain a representation of the isosinglet unpolarized distribution as

$$[u(x)+d(x)]_{\rm nonoccup}=-N_cM_N\sum_{\substack{n\\ \rm nonoccup}}\int\frac{d^3k}{(2\pi)^3}\Phi_n^\dagger(\mathbf{k})(1+\gamma^0\gamma^3)\times\delta(k^3+E_n-xM_N)\Phi_n(\mathbf{k}), \tag{36}$$

which, again, gives minus the antiquark distribution at negative x. In Eq. (35) vacuum subtraction is understood for $x<0$, in Eq. (36) for $x>0$.

The analogous expression for the isovector polarized distribution is

$$[\Delta u(x)-\Delta d(x)]_{\rm occup}=-\frac{1}{3}(2T_3)N_cM_N\sum_{\substack{n\\ \rm occup}}\int\frac{d^3k}{(2\pi)^3}\Phi_n^\dagger(\mathbf{k})\tau^3(1+\gamma^0\gamma^3)\times\gamma_5\delta(k^3+E_n+xM_N)\Phi_n(\mathbf{k}), \tag{37}$$

with the corresponding antiquark distribution given by the same expression with $x\to -x$ (vacuum subtraction is again understood). Here, $2T_3=\pm 1$ for proton and neutron, respectively. The alternative representation as a sum over nonoccupied states analogous to Eq. (36) can easily be written down.

The isovector unpolarized and isosinglet polarized quark distributions vanish in the leading order of the $1/N_c$ expansion. They are nonzero only after considering rotational corrections, i.e., expanding to first order in the soliton angular velocity, which is $O(1/N_c)$, and are expressed as double sums over single-particle levels. We shall not consider them in this paper. We note, however, that the techniques developed in Secs. III and IV can readily be generalized to analyze also these ''small'' distributions.

III. ULTRAVIOLET DIVERGENCES AND REGULARIZATION

The expressions for the quark distribution functions derived in the previous section are ultraviolet divergent and require regularization. To be able to compute the distribution functions using the effective chiral theory we must ensure that the ultraviolet regularization does not lead to violation of any of their fundamental properties. We want to show now that regularization by a Pauli-Villars subtraction, which preserves the completeness of the quark single-particle states in the chiral soliton, leads to regularized quark and antiquark distributions satisfying all general requirements. It was noted in Sec. II that the equivalence of the representations of the distribution functions as sums over occupied and nonoccupied states relies on the completeness of the single-particle states. We shall see below that, with Pauli-Villars regularization, this equivalence is preserved for the regularized distributions. On the other hand, regularizations based on an energy cutoff not only destroy the equivalence of summation over occupied and nonoccupied states, but lead also to other, related, unphysical features.

The divergent contribution in Eq. (35) comes from the eigenstates of the Dirac Hamiltonian with large energy, $|E_n|$. One may think therefore that a natural way to regularize this divergence is simply to cut the contributions of states with $|E_n|$ larger than some cutoff ω_0:

$$[u(x)+d(x)]^{\omega_0}_{\rm occup}=N_cM_N\int_{-\omega_0}^{E_{\rm lev}+0}d\omega\,{\rm Sp}[\,\delta(\omega-H)\times\delta(\omega-xM_N+p^3)(1+\gamma^0\gamma^3)]-(H\to H_0). \tag{38}$$

[Here we have written the sum over states, Eq. (35), as an integral over energy, the integrand being a functional trace involving the Hamiltonian and single-particle momentum operator, p^3 [5]. This form is useful for investigating the ultraviolet asymptotics.] In fact, we shall see below that this regularization is unphysical, leading to a number of problems which are easily cured by turning to the Pauli-Villars regularization. However, two reasons force us to devote some time to the distribution function with the energy cutoff, Eq.

(38). First, in order to see explicitly that the Pauli-Villars subtraction cancels all nonphysical effects, one has to understand precisely what is to be canceled. Second, our numerical method for computing the distribution function (see Sec. IV) involves an energy cutoff in the intermediate stages of the calculation (taken to infinity at the end), so it is essential to know the asymptotic properties of the distributions with energy cutoff.

The ultraviolet divergence of Eq. (38) can be derived using the technique developed in [5]. One replaces the δ function by the imaginary part (discontinuity) of the quark propagator in the background pion field:

$$\delta(\omega-H)=\frac{1}{2\pi i}\left(\frac{1}{\omega-H-i0}-\frac{1}{\omega-H+i0}\right). \tag{39}$$

Writing the quark propagator in the form

$$\frac{1}{\omega-H}=\frac{\omega+H}{\omega^2-H^2}=\frac{\omega+\gamma^0(-i\gamma^k\partial_k+MU^{\gamma_5})}{\omega^2+\partial_k^2-M^2-iM\gamma^k(\partial_k U^{\gamma_5})}, \tag{40}$$

one can expand in derivatives of the soliton field. One finds that only the first term in the derivative expansion is divergent. In this way one easily obtains the logarithmic divergence of the distribution function, Eq. (38), in the limit of large energy cutoff:

$$[u(x)+d(x)]^{\omega_0}_{\rm occup}\sim N_c M_N M^2 \ln\frac{\omega_0}{M}\,\mathrm{sgn}(x)\,\frac{1}{4\pi^2}\int\frac{d^3\mathbf{k}}{(2\pi)^3}\times\theta(k^3-M_N|x|)\,\mathrm{Tr}[\widetilde{U}(\mathbf{k})[\widetilde{U}(\mathbf{k})]^\dagger] \quad \text{for} \quad (\omega_0\to\infty). \tag{41}$$

[Here $\theta(y)$ is the step function.] If the soliton field, $U_c(\mathbf{x})$, is smooth in coordinate space, then its Fourier transform, $\widetilde{U}_c(\mathbf{k})$, decays exponentially for large $|\mathbf{k}|$. This means that, as a function of $|x|$, the integral in Eq. (41) also decays exponentially at large $|x|$. One should keep in mind, however, that the asymptotic formula, Eq. (41), is valid only in the parametric range $x\sim 1/N_c \ll \omega_0/M_N$ and thus does not allow us to draw any conclusions about the behavior of the quark distribution function at larger $|x|$.

It is therefore interesting to derive the UV behavior of the distribution function with energy cutoff at larger values of $|x|$. An asymptotic expansion can be performed in the domain $1/N_c \ll |x| \sim \omega_0/M_N$ by computing the UV divergences of the moments of the distribution function (see the Appendix). The asymptotic behavior is given by

$$[u(x)+d(x)]^{\omega_0}_{\rm occup}\sim N_c M_N^{-1} M^2\,\frac{1}{24\pi^2}\left[\frac{4}{x}\,\delta\left(x+\frac{2\omega_0}{M_N}\right)-\frac{1}{x^2}\,\theta\left(\frac{2\omega_0}{M_N}-|x|\right)\theta(-x)\right]\times\int d^3x\,\mathrm{Tr}[\partial_k U(\mathbf{x})\partial_k U^\dagger(\mathbf{x})] \quad \text{for} \quad 1/N_c\ll|x|\sim\omega_0/M_N. \tag{42}$$

It exhibits at large negative x a rather slow $1/x^2$ decay, up to the point $x=-2\omega_0/M_N$, where it ends with a δ-function peak. One should keep in mind that this δ function appears only in the asymptotic limit $x\sim-\omega_0/M_N\to-\infty$. At large but finite values of $x\sim-\omega_0/M_N$ the delta function in Eq. (42) approximates a narrow peak whose width is much smaller than ω_0/M_N. This ''large negative x'' behavior of the distribution function is an artifact of the energy cutoff. We shall see below that both the $1/x^2$ tail and the delta function cancel in Pauli-Villars regularization.

In the previous section we have shown that the quark distribution functions can be represented in two equivalent forms as a sum over either occupied or nonoccupied quark states. In general, regularization violates this equivalence. Let us regularize the sum over nonoccupied states by an energy cutoff similar to Eq. (38):

$$[u(x)+d(x)]^{\omega_0}_{\rm nonoccup}=-N_c M_N\int_{E_{\rm lev}+0}^{\omega_0}d\omega\,\mathrm{Sp}[\,\delta(\omega-H)\times\delta(\omega-xM_N+p^3)(1+\gamma^0\gamma^3)]-(H\to H_0). \tag{43}$$

One can easily show that this sum over nonoccupied states has the same logarithmic divergence for large ω_0 as the sum over occupied states, Eq. (41). This means that the difference between the two representations of the quark distribution functions remains finite for $\omega_0\to\infty$. The question is whether this finite limit is zero or not. The answer is, surprisingly, no. Moreover, this limit can be computed analytically, using a technique similar to the one described in the Appendix. One finds

$$\lim_{\omega_0\to\infty}\{[u(x)+d(x)]^{\omega_0}_{\rm occup}-[u(x)+d(x)]^{\omega_0}_{\rm nonoccup}\}=N_c M_N M^2\,\frac{1}{4\pi^2}\int\frac{d^3k}{(2\pi)^3}\mathrm{Tr}[\widetilde{U}(\mathbf{k})[\widetilde{U}(\mathbf{k})]^\dagger]\times\ln\frac{|xM_N+k^3|}{|xM_N|}. \tag{44}$$

Thus regularization by an energy cutoff leads to an anomalous difference between summation over occupied and nonoccupied states even in the infinite-cutoff limit.

The deeper reason for the artifacts encountered with the energy cutoff is that this regularization violates the completeness of the set of single-particle quark states. The equivalence of the two representations of the distribution functions as sums over occupied and nonoccupied states relies on the locality of the equal-time anticommutator of quark fields [or, equivalently, of the discontinuity of the Feynman Green function, Eq. (30)]. Leaving out the contribution of high-energy states one is dealing with an incomplete set of quark eigenstates, which results in a modification of the δ-function equal-time anticommutator. In other words, one violates causality, i.e., the anticommutativity of the quark fields at spacelike separations. What is remarkable, though, is that cutoff regularization leads to anomaly-type phenomena which persist even in the infinite-cutoff limit, cf. Eq. (44). Furthermore, Eq. (42) tells us that such regulariza-

tion always leads to unphysical results for the distribution function, no matter which representation of the distribution function one adopts. It should be noted that the usual proper-time regularization of the determinant is of this type.

A regularization which preserves the completeness of states is the Pauli-Villars regularization, where one subtracts from the divergent sums a multiple of the corresponding sums over eigenstates of the Hamiltonian in which the quark mass, M, has been replaced by a regulator mass $M_{\rm PV}$. This mass now plays the role of the physical cutoff of the effective theory, which was denoted generically by Λ in Sec. II. The coefficient of the subtraction is chosen such as to cancel the logarithmic divergence of the distribution function with the energy cutoff, Eq. (41). We thus define

$$[u(x)+d(x)]^{\rm PV}_{\rm occup}(x)=\lim_{\omega_0\to\infty}\left\{[u(x)+d(x)]^{\omega_0}_{\rm occup}(x)\big|_M - \frac{M^2}{M^2_{\rm PV}}[u(x)+d(x)]^{\omega_0}_{\rm occup}(x)\big|_{M_{\rm PV}}\right\}, \tag{45}$$

and similarly for the sum over nonoccupied states. One observes that the unphysical phenomena associated with the energy cutoff—the negative-x behavior, Eq. (42), and the anomalous difference of summing over occupied and nonoccupied states, Eq. (44)—are proportional to the quark mass squared, M^2. Thus, the artifacts of the energy cutoff cancel under the Pauli-Villars subtraction, Eq. (45), as it should be. In particular, the Pauli-Villars regularized distributions can now equivalently be computed as sums over occupied or nonoccupied states.

In this section we have investigated the consequences of ultraviolet regularization on the distribution functions using asymptotic expansion techniques. The physical distributions, for finite Pauli-Villars cutoff, can only be computed numerically. Below we shall see that the numerically computed distribution functions in Pauli-Villars regularization satisfy all general requirements. The distributions decrease rapidly for large $|x|$ and exhibit the correct positivity properties, in full accordance with the results of the asymptotic analysis.

IV. COMPUTATION OF QUARK DISTRIBUTION FUNCTIONS

A. Spherically symmetric representation for distribution functions

We now develop a method for numerical computation of the Pauli-Villars regularized distribution functions. Our general strategy will be as follows. We compute the distribution functions as sums over quark levels, Eqs. (35) and (37), for a large but finite energy cutoff. Such ''intermediate'' regularization is necessary in order to have expressions which can be computed using finite basis methods. The physical distribution functions are then obtained by subtracting the corresponding sums with the PV regulator mass, $M_{\rm PV}$, according to Eq. (45), and removing the energy cutoff by extrapolation to infinity. In this way, the energy cutoff affects only the intermediate steps of the calculation, not the final result.

For intermediate regularization we now introduce an energy cutoff in Eqs. (35) and (37) in the form

$$[u(x)+d(x)]^R_{\rm occup}=N_cM_N\sum_{\substack{n\\ \rm occup}}\langle n|(1+\gamma^0\gamma^3)\times\delta(E_n-xM_N+p^3)|n\rangle R(E_n), \tag{46}$$

$$[\Delta u(x)-\Delta d(x)]^R_{\rm occup}=-\frac{1}{3}(2T_3)N_cM_N\sum_{\substack{n\\ \rm occup}}\langle n|\delta(E_n-xM_N+p^3)\tau^3\times(1+\gamma^0\gamma^3)\gamma_5|n\rangle R(E_n). \tag{47}$$

We have written the matrix elements between single-particle levels in abstract form, with p^3 denoting the z component of the single-particle momentum operator. Here, $R(E_n)$ is a smooth regulator function with a cutoff, $E_{\rm max}$. For example, one may employ a Gaussian

$$R(E_n)=\exp\left(-\frac{E_n^2}{E^2_{\rm max}}\right). \tag{48}$$

Alternatively, one may use a Strutinsky (error function) regulator of the kind described in Ref. [18], which leads to more rapidly converging sums over levels. A corresponding regularization can be introduced also in the sums over nonoccupied states.

Before evaluating the sums over levels, Eqs. (46) and (47), it is convenient to convert them to a more symmetric form. In the derivation of the distribution functions in Sec. II, using the infinite-momentum frame, it was assumed that the nucleon is moving in the z direction. The orientation of the nucleon velocity is, of course, arbitrary, and the distribution functions do not depend on it. We can thus write Eqs. (46) and (47) equivalently as

$$[u(x)+d(x)]^R_{\rm occup}=N_cM_N\sum_{\substack{n\\ \rm occup}}\langle n|(1+\gamma^0\mathbf{v}\cdot\ \gamma)\times\delta(E_n-xM_N+\mathbf{v}\cdot\mathbf{p})|n\rangle R(E_n), \tag{49}$$

$$[\Delta u(x)-\Delta d(x)]^R_{\rm occup}=-\frac{1}{3}(2T_3)N_cM_N\sum_{\substack{n\\ \rm occup}}\langle n|\mathbf{v}\cdot\ \tau(1+\gamma^0\mathbf{v}\cdot\ \gamma)\times\gamma_5\delta(E_n-xM_N+\mathbf{p}\cdot\mathbf{v})|n\rangle R(E_n). \tag{50}$$

where $\mathbf{v}$ is an arbitrary three-dimensional unit vector, $\mathbf{v}^2=1$. For the isosinglet unpolarized distribution this is immediately obvious; in the case of the isovector polarized distribution, Eq. (50), we have made use of the ''hedgehog'' symmetry of the classical meson field, Eq. (6), and the Hamiltonian, Eq. (8), i.e., the invariance under simultaneous rotations in spin and isospin space. We can now pass to a

spherically symmetric representation by averaging over the orientations of $\mathbf{v}$ before computing the sum over quark levels. Using the identity

$$\frac{1}{4\pi}\int d\Omega_v\,\delta(E_n - xM_N + \mathbf{v}\cdot\mathbf{p}) = \frac{1}{2|\mathbf{p}|}\,\theta(|\mathbf{p}| - |E_n - xM_N|), \tag{51}$$

and its generalizations, we rewrite Eqs. (49) and (50) in the form

$$[u(x)+d(x)]^R_{\text{occup}} = N_c M_N \sum_{\substack{n\\ \text{occup}}} \langle n|A^{(1)} + A^{(2)}\gamma^0\mathbf{p}\cdot\boldsymbol{\gamma}|n\rangle R(E_n), \tag{52}$$

$$[\Delta u(x) - \Delta d(x)]^R_{\text{occup}} = -\frac{1}{3}(2T_3)N_c M_N \sum_{\substack{n\\ \text{occup}}} \langle n|A^{(3)}\gamma_5\mathbf{p}\cdot\boldsymbol{\tau} + A^{(4)}\gamma^0\mathbf{p}\cdot\boldsymbol{\gamma}\gamma_5\mathbf{p}\cdot\boldsymbol{\tau} + A^{(5)}\gamma^0\boldsymbol{\tau}\cdot\boldsymbol{\gamma}|n\rangle R(E_n). \tag{53}$$

Here, $A^{(k)}(k=1,\ldots,5)$, are scalar functions of the magnitude of the single-particle momentum operator, $|\mathbf{p}|$, as well as of the level energy, E_n, and x:

$$A^{(k)}(|\mathbf{p}|,E_n,x) = \frac{1}{2|\mathbf{p}|}\,\theta(|\mathbf{p}| - |E_n - xM_N|)\times \begin{cases} 1, & k=1,\\ -\dfrac{(E_n - xM_N)}{|\mathbf{p}|^2}, & 2,\\ -\dfrac{(E_n - xM_N)}{|\mathbf{p}|^2}, & 3,\\ -\dfrac{1}{2|\mathbf{p}|^2} + \dfrac{3}{2}\dfrac{(E_n - xM_N)^2}{|\mathbf{p}|^4}, & 4,\\ \dfrac{1}{2} - \dfrac{1}{2}\dfrac{(E_n - xM_N)^2}{|\mathbf{p}|^2}, & 5. \end{cases} \tag{54}$$

These operator functions of $|\mathbf{p}|$ are understood in the usual sense, as functions of the eigenvalues in a basis where the operator is diagonal.

B. Evaluation in a discrete basis

The distribution functions, Eqs. (52) and (53), are sums of diagonal matrix elements of functions of single-particle operators between eigenstates of the Dirac Hamiltonian in the background pion field, Eq. (8). To evaluate them numerically we employ a basis of eigenfunctions of the free Dirac Hamiltonian:

$$H_0\phi_i = E_i^{(0)}\phi_i,$$
$$H_0 = -i\gamma^0\gamma^k\partial_k + M\gamma^0. \tag{55}$$

The basis is made discrete by placing the soliton in a three-dimensional spherical box of finite radius, imposing the Kahana-Ripka boundary conditions on the surface [12]. The eigenvalues and eigenfunctions of the full Hamiltonian, Eq. (8), are then determined by numerical diagonalization in the discrete basis:

$$\sum_j H_{ij}c_{nj} = E_n c_{ni}, \tag{56}$$

$$H_{ij} = \int_{\text{box}} d^3x\,\phi_i^\dagger(\mathbf{x})H\phi_j(\mathbf{x}), \tag{57}$$

$$\Phi_n(\mathbf{x}) = \sum_i c_{ni}\phi_i(\mathbf{x}). \tag{58}$$

Since the operator $|\mathbf{p}|$ is a function of the free Hamiltonian,

$$|\mathbf{p}| = \sqrt{H_0^2 - M^2}, \tag{59}$$

it is diagonal in the basis of H_0 eigenstates, Eq. (55), and one has

$$\langle i|f(|\mathbf{p}|)|j\rangle = f(|\mathbf{p}|_i)\,\delta_{ij},$$
$$|\mathbf{p}|_i \equiv \sqrt{(E_i^{(0)})^2 - M^2}, \tag{60}$$

for any function, $f(|\mathbf{p}|)$. Using this property one can explicitly evaluate the matrix elements between levels in Eqs. (52) and (53), and obtains

$$[u(x)+d(x)]^R_{\text{occup}} = N_c M_N \sum_{\substack{n\\ \text{occup}}} \sum_{i,j} c_{ni}^* c_{nj} \times [A^{(1)}(|\mathbf{p}|_i,E_n,x)\,\delta_{ij}$$

$$+A^{(2)}(|\mathbf{p}|_i,E_n,x)$$
$$\times(\gamma^0\mathbf{p}\cdot\boldsymbol{\gamma})_{ij}]R(E_n), \tag{61}$$

$$[\Delta u(x)-\Delta d(x)]^R_{\rm occup}$$
$$=-\frac{1}{3}(2T_3)N_cM_N\sum_{\substack{n\\ \rm occup}}\sum_{i,j}c^*_{ni}c_{nj}\Big[A^{(3)}(|\mathbf{p}|_i,E_n,x)$$
$$\times(\gamma_5\mathbf{p}\cdot\boldsymbol{\tau})_{ij}+A^{(4)}(|\mathbf{p}|_i,E_n,x)\sum_k(\gamma^0\mathbf{p}\cdot\boldsymbol{\gamma})_{ik}$$
$$\times(\gamma_5\mathbf{p}\cdot\boldsymbol{\tau})_{kj}+A^{(5)}(|\mathbf{p}|_i,E_n,x)(\gamma^0\boldsymbol{\tau}\cdot\boldsymbol{\gamma})_{ij}\Big]R(E_n). \tag{62}$$

Now the $A^{(k)}$, $(k=1,\ldots,5)$ are ordinary functions of the eigenvalues of $|\mathbf{p}|$ in basis states, $|\mathbf{p}|_i$. Here, $(\ldots)_{ij}$ denote the matrix elements of the corresponding operator between basis states. We remind that the corresponding antiquark distributions are given, respectively, by minus the RHS of Eq. (61) at negative x, and that of Eq. (62) at negative x; see end of Sec. II B.

We note that the Dirac and isospin structures appearing in Eqs. (61) and (62) are essentially the same as those in the sums determining the nucleon mass and isovector axial coupling, $g_A^{(3)}$ [6,7]. To simplify the calculation of the matrix elements one may use that

$$\gamma^0\mathbf{p}\cdot\boldsymbol{\gamma}=H_0-M\gamma^0, \tag{63}$$

and that the operator appearing in the first and second term on the RHS of Eq. (62) can be expressed as an anticommutator:

$$\gamma_5\mathbf{p}\cdot\boldsymbol{\tau}=\frac{1}{2}\{\gamma_5\gamma^0\boldsymbol{\tau}\cdot\boldsymbol{\gamma},\gamma^0\mathbf{p}\cdot\boldsymbol{\gamma}\}. \tag{64}$$

The terms in the sums Eqs. (61) and (62) are proportional to a step function depending on the level energy, E_n, the momenta of the basis states, $|\mathbf{p}|_i$, and the Bjorken variable, x. The expressions can not directly be used for numerical evaluation in a discrete basis, since the result would be a discontinuous function of x. There are, however, ways to convert Eqs. (61) and (62) to a form suitable for evaluation in a discrete basis. One possibility is to apply Gaussian smearing in x to the distribution functions. Let us define

$$D^{\rm smeared}(x)\equiv\frac{1}{\gamma\sqrt{\pi}}\int_{-\infty}^{\infty}dx'\exp\left(\frac{-(x-x')^2}{\gamma^2}\right)D(x'), \tag{65}$$

where $D(x)$ stands for the regularized isosinglet unpolarized or isovector polarized distributions. Here, $\gamma\ll 1$ is a small but finite number. These ''smeared'' distribution functions can now be calculated using Eqs. (61) and (62) with $A^{(k)}$ replaced by the corresponding ''smeared'' functions in x:

$$A^{(k)}(|\mathbf{p}|_i,E_n,x)\to A^{(k)\rm smeared}(|\mathbf{p}|_i,E_n,x). \tag{66}$$

These are now continuous functions of the level momenta and energies, so one may perform the sums over levels in the discrete basis, provided one makes sure that the separation between the momentum eigenvalues of the basis states is significantly smaller than the smearing width, γ. The level spacing is inversely proportional to the size of the Kahana-Ripka box, so it becomes necessary to use rather large boxes to attain small values of γ. In the calculations described in this paper we use a value of $\gamma=0.1$, which requires box sizes $>20M^{-1}$.

In this way one can compute the smeared distribution functions, Eq. (65). At values of x where the exact distributions are smooth the smeared functions provide an excellent approximation to the exact ones. An exception is the isosinglet unpolarized distribution near $x=0$. The exact distribution has a discontinuity at $x=0$, which becomes a smooth crossover of width $\sim 1/\gamma$ in the smeared distribution. It is possible to recover the discontinuity by ''deconvoluting'' the numerically computed smeared distributions. Dividing the Fourier transform in x of the numerically computed smeared distribution by that of the Gaussian, Eq. (65), one can reconstruct the Fourier transform of the exact distribution for values of the argument up to $\sim 1/\gamma$. The exact distribution function itself is then obtained by inverse Fourier transformation, incorporating the known asymptotic behavior of the Fourier transform for large arguments corresponding to a discontinuity at $x=0$.

We thus compute the mode sums for the smeared distributions, Eqs. (61) and (62), for a number of values of the energy cutoff, typically up to $E_{\rm max}\simeq 10\,M$, and also the corresponding sums with the constituent quark mass replaced by the PV regulator mass, $M_{\rm PV}$. We then perform the PV subtraction, Eq. (45), and remove the energy cutoff by numerical extrapolation to $E_{\rm max}\to\infty$ pointwise in x. One computes a least-squares fit of the PV subtracted sums to a constant plus inverse powers of $E_{\rm max}$, for each x. The stability of the extrapolation can be checked by adding more terms to the fit.

In Sec. III we investigated the asymptotic behavior of the distribution functions with an energy cutoff and noted a number of unphysical features, which are removed by the Pauli-Villars subtraction. This can also be seen directly in the numerical calculations. The numerically computed distribution functions for finite energy cutoff, Eqs. (61) and (62), exhibit a ''tail'' at large negative x, which is proportional to M^2, consistent with the asymptotic formula, Eq. (42). (For summation over nonoccupied states, the ''tail'' occurs at positive x.) Moreover, the result for the anomalous difference between summation over occupied and nonoccupied states, Eq. (44), is confirmed by numerical calculations. Thus the numerical results fully support the conclusions of Sec. III.

Given the equivalence of summing over occupied and nonoccupied states in PV regularization, one may choose any of the two representations for the numerical calculations. In practice, it is convenient to compute the quark distributions by summing over occupied states and the antiquark distributions by summing over nonoccupied states. In this way, no vacuum subtraction is required. Furthermore, these sums exhibit asymptotic behavior in the energy cutoff earlier than the respective other representations, making the extrapolation to infinite cutoff more stable.

When computing the isovector polarized distribution one must keep in mind that it is defined as the limit of zero pion mass of the distribution computed for finite pion mass, i.e., for a soliton profile vanishing exponentially at large radii [5]. (The same limit is understood in the definition of the isovector axial coupling, $g_A^{(3)}$.) We thus must carry out the entire calculation described above (that is, summing over quark levels, PV subtraction and extrapolation to $E_{\max}\to\infty$) for $M_\pi\neq 0$, and take the limit $M_\pi\to 0$ by numerical extrapolation at the very end.[2]

The Gaussian smearing, Eq. (65), offers a simple possibility to compute the distribution function directly as a function of x. We note, however, that the use of the spherically symmetric representation, Eqs. (61) and (62), is not limited to this method. In fact, performing other functional transformations of the expressions (61) and (62) before summing over levels one can obtain prescriptions for evaluating the distribution functions in a variety of representations. For example, replacing in Eqs. (61) and (62) the functions $A^{(k)}$ by their moments,

$$A_m^{(k)}(|\mathbf{p}|_i,E_n)=\int_{-1}^{1}dx x^{m-1}A^{(k)}(|\mathbf{p}|_i,E_n,x)$$

$$(m=1,2,\ldots), \tag{67}$$

one obtains a formula for numerical evaluation of the moments of the distribution function. (Again, one must compute the sums for finite energy cutoff, perform the Pauli-Villars subtraction and extrapolate to infinite cutoff.) We have computed the lowest moments of the distributions in this way ($m<10$) and verified that they coincide with the moments of the numerically computed distribution functions.

V. NUMERICAL RESULTS AND DISCUSSION

In the numerical calculations we use the standard value for the constituent quark mass, $M=350$ MeV, as derived from the instanton vacuum [17]. The value of the PV regulator mass, $M_{\rm PV}$, is determined by reproducing the experimental value of the pion decay constant:

$$F_\pi^2=4N_c\int\frac{d^4k}{(2\pi)^4}\frac{M^2}{(M^2+k^2)^2}$$

$$-4N_c\frac{M^2}{M_{\rm PV}^2}\int\frac{d^4k}{(2\pi)^4}\frac{M_{\rm PV}^2}{(M_{\rm PV}^2+k^2)^2}=\frac{N_cM^2}{4\pi^2}\ln\frac{M_{\rm PV}^2}{M^2}. \tag{68}$$

With $F_\pi=93$ MeV one obtains $M_{\rm PV}^2/M^2=2.52$. For the soliton profile, Eq. (6), we use the variational form of Ref. [6],

$$P(r)=-2\arctan\left(\frac{r_0^2}{r^2}\right), \tag{69}$$

[2]If one computed the isovector distribution directly for a massless soliton profile, $P(r)\sim 1/r^2$ for $r\to\infty$, one would find a singularity at $x=0$ (regulated only by the finite box size). The distribution obtained as a limit of a massive profile is nonsingular at $x=0$.

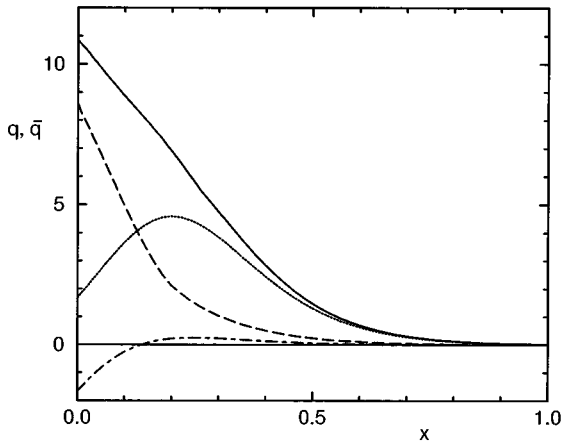

FIG. 1. The isosinglet unpolarized quark and antiquark distributions. *Solid line:* quark distribution, $u(x)+d(x)$, total result (discrete level plus Dirac continuum); *dotted line:* contribution of the discrete level (after PV subtraction) to $u(x)+d(x)$. *Dashed line:* antiquark distribution, $\overline{u}(x)+\overline{d}(x)$, total result; *dot-dashed line:* contribution of the discrete level to $\overline{u}(x)+\overline{d}(x)$.

with $r_0=1.0M^{-1}$, which gives a reasonable description of a varitey of hadronic observables of the nucleon. For these parameters, the nucleon mass is found to be $M_N=1150$ MeV. [The nucleon mass is also computed in PV regularization, subtracting from Eq. (9) $M^2/M_{\rm PV}^2$ times the corresponding expression for the Hamiltonian with $M_{\rm PV}$. The contribution of the discrete level is also subtracted.] For calculation of the isovector polarized distribution, we introduce a finite pion mass in Eq. (69) in the form

$$P_{M_\pi}(r)=-2\arctan\left[\frac{r_0^2}{r^2}(1+M_\pi r)\exp(-M_\pi r)\right]. \tag{70}$$

This form has the correct Yukawa tail at large r but is not modified compared to Eq. (69) at $r=0$. The limit $M_\pi\to 0$ is taken at the very end of the calculation.

The result for the isosinglet unpolarized quark and antiquark distributions is shown in Fig. 1. For both distributions we show separately the total result (the sum of the discrete level and the negative Dirac continuum) and the contribution of the discrete level. One sees that the discrete level contributes to the antiquark distribution with a negative sign. [The contribution of the discrete level to the RHS of Eq. (61) is continuous at $x=0$, and the antiquark distribution is just given by the negative of Eq. (61) at negative x.] An approximation in which only the discrete level is taken into account would thus lead to negative antiquark distributions [19]. Positivity of the antiquark distribution is naturally restored by including the Dirac continuum. This is clear in the light of the discussion of Sec. III: Restricting oneself to the contribution of the discrete level one is working with an incomplete set of states. Only the sum of all levels (discrete plus Dirac continuum) gives the correct realization of the distribution function in the effective theory.

The result for the isovector polarized quark and antiquark distributions is displayed in Fig. 2 (total results and level contributions). One again observes a sizable contribution

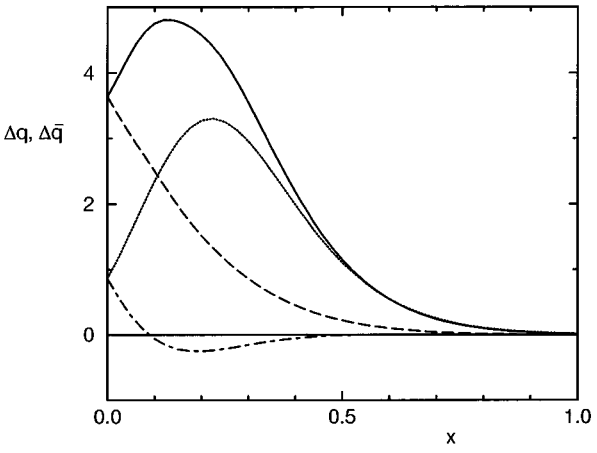

FIG. 2. The isovector polarized quark and antiquark distributions. *Solid line:* quark distribution, $\Delta u(x)-\Delta d(x)$, total result (discrete level plus Dirac continuum); *dotted line:* contribution of the discrete level (after PV subtraction) to $\Delta u(x)-\Delta d(x)$. *Dashed line:* antiquark distribution, $\Delta\overline{u}(x)-\Delta\overline{d}(x)$, total result; *dot-dashed line:* contribution of the discrete level to $\Delta\overline{u}(x)-\Delta\overline{d}(x)$.

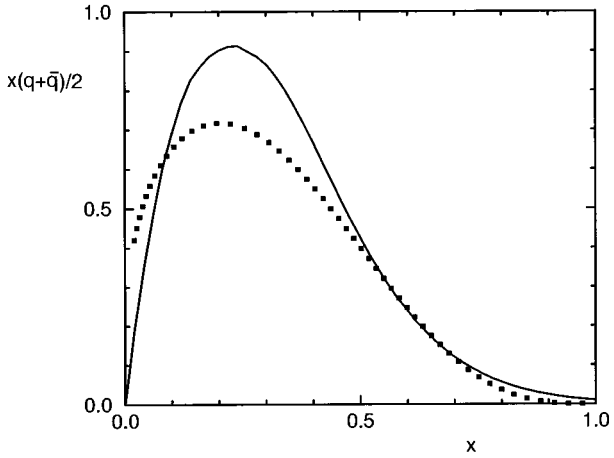

FIG. 3. The isosinglet unpolarized distribution of quarks plus antiquarks, $\frac{1}{2}x[u(x)+d(x)+\overline{u}(x)+\overline{d}(x)]$. *Solid line:* calculated distribution (total result, cf. Fig. 1). *Points:* NLO parametrization of Ref. [3].

from the Dirac continuum, which reverses the sign of the level contribution to the antiquark distribution. Here, however, contrary to the isosinglet unpolarized distribution, no definite sign is required *a priori*.

The calculated distributions should in principle be used as input for perturbative evolution, starting with a scale of the order of the cutoff, $M_{\rm PV}\simeq 600$ MeV. We stress that we are computing the twist-2 parton distributions at a low normalization point, not the structure function (cross section) at low q^2, so a meaningful comparison with the data can be performed only after evolution to large q^2. Alternatively, we may compare our calculations with the parametrizations of Glück and co-workers [3,4]. Starting from ''valencelike'' (nonsingular) quark, antiquark, and gluon distributions at a normalization point well below 1 GeV, these authors can fit at large q^2 not only all the data in the large-x region, but also the recent small-x data down to $x\sim 10^{-4}$. We emphasize that the quark and antiquark distributions obtained in our approach are precisely of this ''valencelike'' form. Moreover, the normalization points of the leading order (LO) and next LO (NLO) distributions of [3,4] are close to our cutoff, so one may perform a preliminary comparison without taking into account evolution.

Figure 3 shows the isosinglet unpolarized total distribution (quarks plus antiquarks) together with the fits of [3]. Our distribution is larger than that of [3] since their fit includes gluons, which carry about 30% of the nucleon momentum at this scale. For the variational soliton profile, Eq. (69), the second moment of the calculated distribution of quarks plus antiquarks is 0.8. (With a self-consistent solution it would be unity, since the energy momentum sum rule follows from the equations of motion for the pion field [5].)

The isosinglet unpolarized valence quark distribution (quarks minus antiquarks) is compared in Fig. 4. Here we have taken in our calculation $M_{\rm PV}\to\infty$, since this distribution function is ultraviolet finite and should not be regularized in order to preserve the baryon number sum rule. It is interesting to see how this sum rule is realized in the large-N_c approach. In fact, the (unregularized) contribution of each level to the baryon number is N_c, as can be seen, for instance, by integrating Eq. (52) over both negative and positive x. Since the baryon number of the discrete level is N_c, the contribution of the negative Dirac continuum to the baryon number must be zero in order to satisfy the sum rule for the total distribution. Indeed, one observes that the baryon number of the negative continuum vanishes when the cutoff is taken to infinity. However, this does not mean that the Dirac continuum does not contribute to the valence quark distribution—just the integral of its contribution is zero. In Fig. 4 we show both the total result (discrete level plus continuum) and the continuum contribution, which integrates to zero.

The isovector polarized total distribution (quarks plus antiquarks) is shown in Fig. 5. The calculated distribution is systematically smaller than the fit of [4]. This is related to

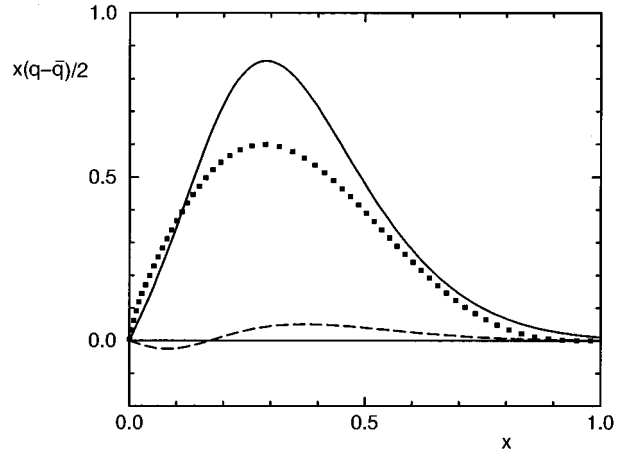

FIG. 4. The isosinglet unpolarized valence quark distribution, $\frac{1}{2}x[u(x)+d(x)-\overline{u}(x)-\overline{d}(x)]$. *Solid line:* calculated distribution (total result); *dashed line:* contribution of the Dirac continuum. *Points:* NLO parametrization of Ref. [3].

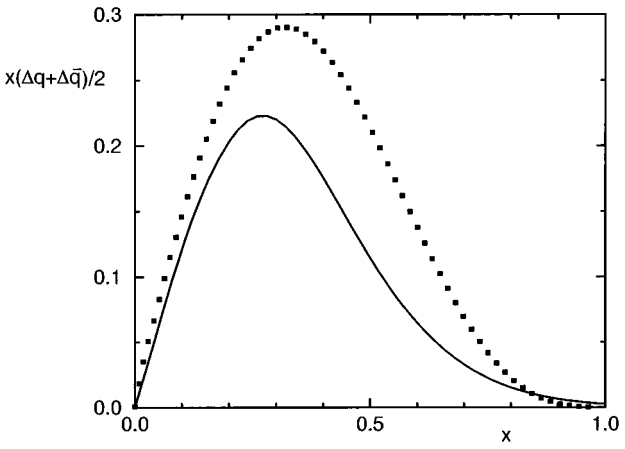

FIG. 5. The isovector polarized distribution of quarks plus antiquarks, $\frac{1}{2}x[\Delta u(x)-\Delta d(x)+\Delta\overline{u}(x)-\Delta\overline{d}(x)]$. *Solid line:* calculated distribution (total result, cf. Fig. 2). *Points:* NLO parametrization of Ref. [4].

the fact that the isovector axial coupling, $g_A^{(3)}$, which determines the normalization of this distribution, is underestimated in the leading order of the $1/N_c$ expansion (with our parameters for the chiral soliton we obtain $g_A^{(3)}=0.9$). We note that $1/N_c$ corrections to this quantity have been computed [20]; the same techniques could also be applied to the distribution functions. In Fig. 6 we show the polarized antiquark distribution, which was assumed to be zero in the fit of [4]. In our calculation it is obtained nonzero, however, significantly smaller than the total distribution of quarks plus antiquarks.

To summarize, we obtain a reasonable description of the isosinglet unpolarized and isovector polarized quark and antiquark distributions. In particular, we find a large antiquark distribution at the low normalization point, in agreement with the parametrizations of the data.

In the calculations reported here we have chosen the variational soliton profile, Eq. (69), with a radius which

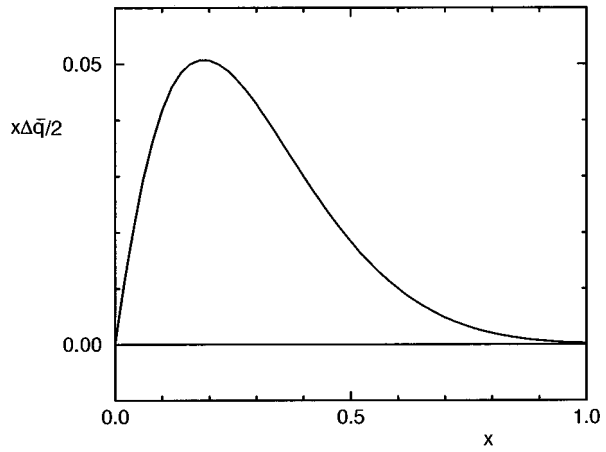

FIG. 6. The isovector polarized antiquark distribution, $\frac{1}{2}x[\Delta\overline{u}(x)-\Delta\overline{d}(x)]$. *Solid line:* calculated distribution (total result, cf. Fig. 2). In the fit of Ref. [4] this distribution is assumed to be zero.

gives a reasonable overall description of a number of hadronic observables, for example the $N\Delta$ splitting [6]. In principle, the classical pion field describing the nucleon should be determined as the minimum of the static energy, i.e., as the self-consistent solution of the equations of motion of the pion field. The calculation of parton distributions with the self-consistent pion field will be the subject of a separate investigation.

The exact numerical calculations fully support the approximation used in [5], based on the ''interpolation formula'' for the quark propagator in the background pion field. For both unpolarized and polarized distributions the differences to the exact results are of the order of 10% for the total distributions (quarks plus antiquark), somewhat larger for quarks and antiquarks separately.

VI. CONCLUSIONS

In this paper we have completed the first part of the program formulated in [5]. We have computed the leading quark distribution functions in the $1/N_c$ expansion, namely the isosinglet unpolarized and isovector polarized, in the effective chiral theory.

Starting from the original definition of parton distributions as numbers of particles carrying fraction x of the nucleon momentum in the infinite-momentum frame, we have shown that it leads in the large-N_c limit to the same results as the QCD definition of distribution functions as matrix elements of bilinears of quark fields on the light cone. The fact that the equivalence of the two definitions of distribution functions can be established within the mean-field picture at large N_c shows the scope of this relativistically covariant, field-theoretical description of the nucleon.

We have observed that, generally speaking, the calculation of quark distribution functions puts strong demands on the regularization of the effective theory. A crucial requirement is that it should preserve the completeness of the basis of single-particle quark wave functions in which one expands the fermion fields in the mean-field approximation. A regularization by subtraction, such as the Pauli-Villars regularization, meets this requirement, while methods based on an energy (or other) cutoff violate this completeness, and thus, causality. In particular, the anomaly observed in the difference of summation over occupied and nonoccupied states in Sec. III shows that one faces here a truly qualitative difference between regularization methods, not simply finite-cutoff effects vanishing in the infinite-cutoff limit. By explicit calculation, we have shown that Pauli-Villars regularization leads to quark and antiquark distributions satisfying all general requirements.

As to the numerical calculations, we have presented a general scheme for computing the distribution functions in various representations. It is remarkable that the Kahana-Ripka method, using a basis of eigenstates of the free Hamiltonian, lends itself so naturally to the computation of distribution functions after one has converted them to a spherically symmetric form.

The methods developed here, both analytical and numerical, can readily be generalized to compute also the ''small'' quark distributions in the $1/N_c$ expansion, the isovector unpolarized and isosinglet polarized distributions. They are

given by double sums over quark levels in the background pion field (formulas have been presented in [5]). Calculations of these distributions are in progress.

We have found reasonable agreement of our results with the fits of Glück and co-workers [3,4]. Indeed, the large-N_c approach to parton distributions formulated in [5] provides justification for the picture of ''valencelike'' distributions at a low normalization point. The fact that at large N_c the nucleon is characterized by a classical pion field (or, equivalently, a polarized Dirac sea of quarks) naturally explains the large antiquark content at the low normalization point. The antiquark distributions obtained in our approach are nonsingular at small x. We note also that the parametric suppression of the gluon relative to the quark distributions, which is implied by the effective chiral theory (see Sec. I and Ref. [5]), seems not to be in contradiction with the parametrization of the data at low normalization point [3]. A 30% momentum fraction of gluons at the low normalization point is consistent with the suppression of the gluon distribution by M^2/Λ^2. However, in order to make this more quantitative one should develop this approach to a level which allows one to compute a nonzero gluon distribution. This can be done in the framework of the instanton vacuum, using the methods of [8].

ACKNOWLEDGMENTS

This work has been supported in part by the NATO Scientific Exchange Grant No. OIUR.LG 951035, by INTAS Grants Nos. 93-0283 EXT and 93-1630-EXT, by a joint grant of the Deutsche Forschungsgemeinschaft and the Russian Foundation for Basic Research, and by COSY (Jülich). The Russian participants acknowledge the hospitality of Bochum University. P.V.P. and M.V.P. are supported by the A.v. Humboldt Foundation. It is a pleasure to thank Klaus Goeke for encouragement and multiple help.

APPENDIX: ASYMPTOTICS FOR LARGE ENERGY CUTOFF

In this appendix we discuss the asymptotic properties of the distribution function with the energy cutoff, which was introduced in Sec. III as a device to control the intermediate steps of the calculation. In particular, we show how the large-x asymptotic behavior, Eq. (42), can be derived. This formula assumes the double limit of large x (in the sense of $N_c x \gg 1$) and large energy cutoff ($\omega_0 \gg M$). It is convenient to analyze this limit in terms of the moments of the distribution functions. An explicit expression for the moments is obtained by integrating Eq. (38) over x,

$$M_n^{\omega_0} = \int_{-1}^{1} dx x^{n-1} [u(x)+d(x)]_{\rm occup}^{\omega_0}$$
$$= N_c M_N^{1-n} \int_{-\omega_0}^{E_{\rm lev}+0} d\omega \,{\rm Sp}[\,\delta(\omega - H)(\omega + p^3)^{n-1}$$
$$\times (1+\gamma^0\gamma^3)] - (H \to H_0) \quad (n = 1,2,\ldots). \tag{A1}$$

The delta function of the Hamiltonian can be represented as the discontinuity of the quark propagator, cf. Eq. (39). One obtains a representation of the moments as

$$M_n^{\omega_0} = -\frac{i}{2\pi} \int_0^{\omega_0} d\omega' [\,\widetilde{M}_n(-i\omega'+0) - \widetilde{M}_n(-i\omega'-0)], \tag{A2}$$

where

$$\widetilde{M}_n(\omega) = -iN_c M_N^{1-n} {\rm Sp}\left[\frac{1}{-\omega + iH} (-i\omega + p^3)^{n-1} \right.$$
$$\left. \times (1+\gamma^0\gamma^3) \right] - (H \to H_0). \tag{A3}$$

The integrand of Eq. (A1) is ultraviolet finite for any fixed ω, and an ultraviolet divergence appears in Eq. (A1) only in the limit $\omega_0 \to \infty$ due the large-ω behavior of the integrand (typically a powerlike growth; see below). Equation (A3), on the other hand, contains ultraviolet divergences even for fixed ω due to large momenta. The difference is that in Eq. (A1) we have the delta function of the Hamiltonian, which constrains the ultraviolet growth of the integrand. We therefore have to introduce an additional regularization of the functional trace in Eq. (A3) at fixed ω. The dependence on this additional cutoff cancels, however, after taking the discontinuity in Eq. (A2), and thus does not influence the final result.

Writing the propagator as in Eq. (40) one can expand Eq. (A3) in derivatives of the pion field:

$$\widetilde{M}_n(\omega) = \sum_{k=1}^{\infty} \widetilde{M}_n^{(k)}(\omega), \tag{A4}$$

$$\widetilde{M}_n^{(k)}(\omega) = (-i)^n N_c M_N^{1-n}$$
$$\times {\rm Sp}\left\{ \frac{1}{\omega^2 - \partial_k^2 + M^2} \left[M(\partial\!\!\!/ U^{\gamma_5}) \frac{1}{\omega^2 - \partial_k^2 + M^2} \right]^k \right.$$
$$\times (-i\omega\gamma_0 - \gamma_k\partial_k + iMU^{-\gamma_5})(\omega + \partial_3)^{n-1}$$
$$\left. \times (-i\omega\gamma_0 + \gamma_3) \right\}. \tag{A5}$$

For the calculation of the leading large-x asymptotics it is sufficient to restrict oneself to the first two terms in Eq. (A4). The traces are easily evaluated by inserting plane-wave states:

$$\widetilde{M}_n^{(k)}(\omega) = 4M^2 N_c M_N^{1-n} \int \frac{d^3p}{(2\pi)^3} \int \frac{d^3q}{(2\pi)^3}$$

$$\times \mathrm{Tr}[\widetilde{U}(\mathbf{p})[\widetilde{U}(\mathbf{p})]^{\dagger}] \frac{1}{[\omega^2+(\mathbf{p}-\mathbf{q})^2+M^2]} \times \begin{cases} \dfrac{p^3(-i\omega+q^3)^{n-1}}{(\omega^2+|\mathbf{q}|^2+M^2)}, & k=1, \\ \dfrac{(-i\omega+q^3)^n|\mathbf{p}|^2}{(\omega^2+|\mathbf{q}|^2+M^2)^2}, & k=2. \end{cases} \tag{A6}$$

The integral over q is divergent, but, as said above, the divergent terms do not contribute to the discontinuity in ω. Keeping only those terms that lead to the discontinuity we obtain

$$\widetilde{M}_n^{(k)}(\omega) = 4M^2 N_c M_N^{1-n}(-i)^{n+2}\omega^{n-3}\mathrm{sgn}(\mathrm{Re}\,\omega) \times \int d^3x \mathrm{Tr}[\partial_k U(\mathbf{x})\partial_k U^{\dagger}(\mathbf{x})] \times \begin{cases} \dfrac{1}{32\pi}\left[2^{n-2}(n-2)-\dfrac{1}{2}\delta_{n,1}\right], & k=1, \\ \dfrac{1}{48\pi}\left[2^{n-3}(n-1)+\dfrac{1}{2}\delta_{n,2}\right], & k=2. \end{cases} \tag{A7}$$

Inserting this asymptotic behavior in Eq. (A2) we obtain the leading divergences of the moments for $\omega_0 \to \infty$:

$$M_n^{\omega_0} \sim M^2 N_c M_N^{-1} \int d^3x \mathrm{Tr}[\partial_k U(\mathbf{x})\partial_k U^{\dagger}(\mathbf{x})] \times \begin{cases} (-1)^n \dfrac{1}{48\pi^2}\left(\dfrac{2\omega_0}{M_N}\right)^{n-2}\left[8+\dfrac{2}{n-2}\right], & n \geqslant 3, \\ \dfrac{1}{12\pi^2}\ln\omega_0, & n=2. \end{cases} \tag{A8}$$

Thus the moments for $n \geqslant 3$ have power divergences with the energy cutoff, while for $n=2$ the divergence is logarithmic.

The asymptotic behavior of the moments may be expressed in the form of a function of x, assuming that $1/N_c \ll |x| \sim \omega_0/M_N$. Computing the moments of the function of Eq. (42) one may easily check that it corresponds to the large-ω_0 behavior of the $n>3$ moments, Eq. (A8).

To conclude, we have shown that, with an energy cutoff, the moments of the distribution function generally have power divergences. These manifest themselves not in a power divergence of the distribution function at fixed x, but in the occurrence of a ''tail'' at large negative x (large positive x in the case of summation over nonoccupied states). The power divergences are artifacts of the energy cutoff and cancel under the Pauli-Villars subtraction, Eq. (45). The physical, Pauli-Villars regularized distribution functions are well localized in x.

[1] For a review, see A. D. Martin, Acta Phys. Pol. B **27**, 1287 (1996); A. D. Martin, R. G. Roberts, and W. J. Stirling, Phys. Lett. B **354**, 155 (1995); Phys. Rev. D **50**, 6734 (1994).

[2] CTEQ collaboration, H. L. Lai *et al.*, Phys. Rev. D **55**, 1280 (1997); **51**, 4763 (1995).

[3] M. Glück, E. Reya, and A. Vogt, Z. Phys. C **67**, 433 (1995).

[4] M. Glück, E. Reya, M. Stratmann, and W. Vogelsang, Phys. Rev. D **53**, 4775 (1996).

[5] D. I. Diakonov, V. Yu. Petrov, P. V. Pobylitsa, M. V. Polyakov, and C. Weiss, Nucl. Phys. **B480**, 341 (1996).

[6] D. I. Diakonov, V. Yu. Petrov, and P. V. Pobylitsa, Nucl. Phys. **B306**, 809 (1988).

[7] For a review, see Ch. V. Christov *et al.*, Prog. Part. Nucl. Phys. **37**, 91 (1996).

[8] D. Diakonov, M. Polyakov, and C. Weiss, Nucl. Phys. **B461**, 539 (1996).

[9] For a review, see R. L. Jaffe, Talk given at Ettore Majorana International School of Nucleon Structure: 1st Course: The Spin Structure of the Nucleon, Erice, Italy, 1995 [MIT Report No. MIT-CTP-2506, hep-ph/9602236 (unpublished)].

[10] M. Anselmino, A. Efremov, and E. Leader, Phys. Rep. **261**, 1 (1995).

[11] R. P. Feynman, *Photon-Hadron Interactions* (Benjamin, New York, 1972).

[12] S. Kahana and G. Ripka, Nucl. Phys. **A429**, 462 (1984).

[13] E. Witten, Nucl. Phys. **B223**, 433 (1983).

[14] G. Adkins, C. Nappi, and E. Witten, Nucl. Phys. **B228**, 552 (1983).

[15] D. Diakonov and M. Eides, JETP Lett. **38**, 433 (1983).

[16] A. Dhar, R. Shankar, and S. Wadia, Phys. Rev. D **31**, 3256 (1985).

[17] D. Diakonov and V. Petrov, Nucl. Phys. **B272**, 457 (1986); *Hadron Matter Under Extreme Conditions* (Naukova Dumka, Kiew, 1986); p. 192.

[18] L. Vepstas and A. D. Jackson, Phys. Rep. **187**, 109 (1990).

[19] H. Weigel, L. Gamberg, and H. Reinhardt, Phys. Lett. B **399**, 287 (1997); Phys. Rev. D **55**, 6910 (1997).

[20] Ch. V. Christov *et al.*, Phys. Lett. B **325**, 467 (1994); M. Wakamatsu and T. Watabe, *ibid.* **312**, 184 (1994).